



1 **LAND-SE: a software for landslide statistically-based** 2 **susceptibility zonation, Version 1.0**

3

4 **Mauro Rossi and Paola Reichenbach**

5 CNR IRPI, via Madonna Alta 126, 06128 Perugia, Italia

6 Correspondence to: Mauro Rossi (mauro.rossi@irpi.cnr.it)

7

8 **Abstract**

9 Landslide susceptibility (LS) provides an estimate of the landslide spatial occurrence based on
10 local terrain conditions. LS has been evaluated in many locations around the world since the
11 early '80 using distinct modelling approaches, diverse combination of variables, and different
12 partition of the territory (mapping units). Among the different methods, statistical models have
13 been largely used to assess LS and several model types have been proposed in the literature. A
14 recent literature review revealed that authors not always present a complete and comprehensive
15 assessment of the LS that includes model performance analysis, prediction skills evaluation and
16 estimation of the errors and uncertainty.

17 The aim of this paper is to describe LAND-SE (LANDslide Susceptibility Evaluation), software
18 that performs susceptibility modelling and zonation using statistical models, quantifies the
19 model performances and the associated uncertainty. The software is implemented in R, a free
20 software environment for statistical computing and graphics. This provides users with the
21 possibility to implement and improve the code with additional models, evaluations tools or
22 output types. The paper describes the software structure, explains input and output, illustrates
23 specific applications with maps and graphs. The LAND-SE script is delivered with a basic user
24 guide and three example datasets.

25

26 **Keywords:** Landslides, susceptibility, statistical models, zonation, R



27 1 Introduction

28 Landslide susceptibility (LS) is the likelihood of a landslide occurring in an area based on local
29 terrain conditions (Brabb, 1984). In mathematical language, LS quantifies the spatial
30 probability of landslides occurrence in a mapping unit, not considering the temporal probability
31 of failure or the magnitude of the expected landslides. Landslide susceptibility has been
32 evaluated in many locations around the world since the early '80. Authors have evaluated LS
33 using different partition of the territory as mapping units, diversified combination of
34 explanatory variables and distinct methods. Methods for the LS evaluation and mapping can be
35 broadly grouped in: geomorphological mapping, analysis of landslide inventories, heuristic or
36 index-based methods, statistically based models and geotechnical or physically based models
37 (Guzzetti et al., 1999). Among the different approaches, the statistical models have been largely
38 used to assess LS. A recent revision of papers on statistical models (Malamud et al., 2014),
39 have shown that more than 95 different model types were proposed in the literature. Malamud
40 co-authors grouped them in 20 classes, with the most frequent corresponding to logistic
41 regression, neural networks and data overlay. The relevant number of statistical models
42 described in the literature is probably related to the recent increasing number of commercial
43 and open source packages for statistical analysis that can combine and integrate geographical
44 data and/or Open Source GIS (i.e. SAGA GIS, GRASS GIS). The review analysis also revealed
45 that authors not always present a complete and comprehensive assessment of the models
46 performance and prediction skills evaluations and estimation of the errors and uncertainty.
47 Since the large variety of applications of statistical approaches, but the scarcity of model
48 evaluation and quantification of the errors, we have implemented LAND-SE (LANDslide
49 Susceptibility Evaluation), software developed to prepare landslide susceptibility models and
50 zonation at basin and regional scale, with specific functions focused to results evaluation and
51 uncertainty estimation. The software is implemented in R, a free software environment for
52 statistical computing and graphics (R Core Team, 2015). This provides users with the
53 possibility to implement and improve the code with additional models, evaluations tools or
54 output types.

55 The paper describes LAND-SE structure, explains input and output, illustrates with maps and
56 graphs, some applications and provides a basic user guide. It is out of the scope of the
57 manuscript, the description of the characteristics of each model, the advantage/disadvantage of
58 the model evaluation parameters and the analysis of the model results. We have introduced a



59 test area only to show and demonstrate possible potential applications and different output of
60 LAND-SE.

61 The manuscript is structured as follows: section 2 describes the software, its modelling
62 approaches and the main output types; section 3 illustrates the test area and describes some
63 applications and section 4 formalizes some final remarks. The paper is completed by ancillary
64 materials containing the software code, a user guide and example datasets.

65 **2 Software description**

66 LAND-SE, software for landslide susceptibility modelling and zonation was implemented and
67 improved with respect to the code proposed by Rossi and co-authors in 2010. The new version
68 is coded in R (R Core Team, 2015) and it is open source. The software holds on the possibility
69 to perform and combine different statistical susceptibility modelling, evaluate the results and
70 estimate the associated uncertainty. As compared to the previous version (Rossi et al., 2010),
71 the main improvements are related to: i) the possibility to use different cartographic units (pixel-
72 based vs polygon-based); ii) the capacity to perform different type of validation analyses
73 (spatial, temporal, random); iii) the ability to evaluate the model prediction skills and
74 performances using success and prediction rate curves (Chung and Fabbri, 1999; 2003); iv) the
75 possibility to provide results in standard geographical formats (shapefiles, geotiff); v) an
76 optimization and stabilization of the modelling algorithms; vi) the possibility to use additional
77 computational parameters to tune the calculation procedure, for the analysis of large dataset.
78 This software version presents a relevant computer code restructuring (code refactoring),
79 allowing the implementation of new single statistical approaches (e.g. support vector machines,
80 regression tree based approaches) that can be added as new modules, preserving the basic
81 software structure. The new structure simplifies the maintainability and improvement of the
82 source code.

83 Figure 1 shows the logical schema of LAND-SE subdivided in the following five functions:

- 84 I. Data input preparation;
- 85 II. Single susceptibility models and zonation;
- 86 III. Combination of single models using a logistic regression approach;
- 87 IV. Evaluation of single and combined LS models;
- 88 V. Estimation of uncertainty of single and combined LS models.



89 **2.1 Data input preparation**

90 The input data preparation, follows two steps: i) the choice of the cartographic unit and ii) the
91 selection of the criteria for the definition of the training and the validation dataset.

92 LAND-SE is designed to use different cartographic units, reducible to pixels or to polygon-like
93 subdivisions (e.g. slope units, geomorphological subdivisions, administrative boundaries, etc.).
94 The input data shall be provided in tabular format where each line represents one mapping unit
95 with the associated attributes. Since raster data cannot be used directly as input, a preliminary
96 conversion is required to perform the pixel-based analysis.

97 To identify and separate the training and the validation dataset, different criteria can be adopted.
98 Temporal, spatial or random subdivisions can be selected guiding the type of validation
99 analysis. When the temporal validation is selected, secondary information not used in the model
100 training must be provided for the area under analysis. Adopting a temporal subdivision
101 approach, the training and the validation set are composed by the same mapping units and the
102 analysis is performed using the same explanatory variables but different grouping variable (e.
103 g. a different landslide inventory map, often more recent than what is used during the training
104 phase). Differently, in the spatial and random approach, the training and the validation dataset
105 contain different mapping units, characterized by different grouping and explanatory variables.
106 The main difference between the spatial and the random validation is the method chosen to
107 separate the training and the validation dataset: in the first case, the datasets are spatially
108 different (the two areas can be contiguous or not), in the second the subdivision is performed
109 using a random selection. For the pixel-based approach, the definition of the training and the
110 validation dataset can follow the same criteria, but in the literature, the subdivision is commonly
111 performed using a random selection (Van Den Eeckhaut et al., 2010; Felicísimo et al., 2013;
112 Petschko et al., 2014).

113 **2.2 Single susceptibility models estimation (single susceptibility maps)**

114 LAND-SE uses different supervised multivariate statistical models to evaluate the landslide
115 spatial probability, identifying and quantifying the relation between dependent and independent
116 variables. According to previous studies (Carrara et al., 1991; Rossi et al., 2010; Guzzetti et al.,
117 2006, 2012), dependent variable (or grouping variable) is computed as the absence/presence of
118 landslides in the mapping units and is usually derived from a landslide inventory. The
119 independent variables (explanatory variables) are obtained from available thematic information



(morphometry, land cover/use, lithology, etc.). Each model is executed in two phases: a the training phase, where the model reconstructs the relationships between the dependent and the independent variables, and a validation phase, where these relationships are verified in different conditions. LAND-SE calculates landslide susceptibility with the following single models (Rossi et al., 2010): i) linear discriminant analysis (LDA) (Fisher, 1936; Brown, 1998; Venables and Ripley, 2002), ii) quadratic discriminant analysis (QDA) (Venables and Ripley, 2002), iii) logistic regression (LR) (Cox, 1958; Brown, 1998; Venables and Ripley, 2002), and iv) neural network (NN) modelling (Ripley, 1996; Venables and Ripley, 2002). The logistic regression model was significantly improved with respect to Rossi et al. (2010), substituting the previous code based on the “Zelig” package (Owen et al., 2013), with a more stable and performing code based on the “glm” function, included in the well tested base R implementation (R Core Team, 2015).

2.3 Combined model using a logistic regression approach (combined susceptibility maps)

Similarly to the previous version, LAND-SE uses a combination model (CM) based on a logistic regression approach, where the grouping variable is the presence or absence of landslides in the mapping units, and the explanatory variables are the forecasts of the selected single susceptibility models (Rossi et al., 2010). Similarly, to the single logistic regression model, the original code based on the “Zelig” package was substituted with the “glm” function. LAND-SE allows to enable or not, the execution of the combined model selecting different combinations of single models.

2.4 Susceptibility model evaluation

In the training phase, LAND-SE reconstructs the relationships between dependent and independent variables and evaluates the prediction skills of single and combined models (i.e. the capability to predict the original data). In the validation phase, LAND-SE verifies the results in different conditions and evaluates the models capability to predict independent data. Models output of both phases are evaluated using the same tools and in particular the following statistical metrics and indices:

- The dependence among explanatory variables (Belsley, 1991; Hendrickx, 2012);
- Contingency tables (i.e. confusion matrixes) (Jolliffe and Stephenson, 2003);



- 150 • Contingency plots or fourfold plots summarizing the mapping units correctly and
 - 151 incorrectly classified by the models (Jolliffe and Stephenson, 2003);
 - 152 • Error maps showing the geographical distribution of the mapping units correctly and
 - 153 incorrectly classified by the models (Rossi et al., 2010);
 - 154 • Plots showing receiver operating characteristic (ROC) curves (Green and Swets, 1966;
 - 155 Mason and Graham, 2002; Fawcett, 2006) and the associated Area Under Curve (AUC)
 - 156 statistics;
 - 157 • Evaluation plots showing the variation of the sensitivity (“hit rate”), the specificity (1-
 - 158 false positive rate), and of the Cohen's kappa index (Cohen, 1960);
 - 159 • Success and prediction rate curves (Chung and Fabbri, 1999; 2003)
- 160 The description and discussion of the characteristics, advantage/drawbacks of these statistical
- 161 metrics/indices are out of the scope of the manuscript and they will not be described in detail.

162 **2.5 Uncertainty evaluation (single and combined susceptibility zonations)**

163 For each single and combined model, LAND-SE evaluates and quantifies the uncertainty

164 adopting a “bootstrapping” re-sampling technique (Efron, 1979; Davison and Hinkley, 2006).

165 In the training phase, a user-specified number of runs are performed varying the selected

166 dataset. Descriptive statistics for the probability (susceptibility) estimates, including the mean

167 (μ) and the standard deviation (σ), are obtained from an ensemble of model runs (i.e. a user-

168 defined number of LAND-SE simulations are executed to obtain the two descriptive statistics).

169 Such information is portrayed in plots showing estimates for the model uncertainty in each

170 mapping unit and in maps showing the geographical distribution of the uncertainty (Guzzetti et

171 al., 2006; Rossi et al., 2010). To model the uncertainty associated to each LS zonation, the mean

172 and the standard deviation are fitted using a parabolic function (Figure 3D). Such function is

173 used to estimate the uncertainty in the validation phase. The map showing the geographical

174 distribution of the uncertainty can provide additional and relevant information for the use of LS

175 zonation in environmental planning studies. A proper interpretation of the map may provide for

176 each mapping unit a proxy of a degree of confidence associated to the LS estimate.

177 **2.6 SW output formats**

178 LAND-SE can be executed in two different modes: the *standard* that provides textual and

179 graphical results stored respectively in .txt and .pdf, and the *geomode* providing also



geographical output as shapefiles and GeoTIFF. Some output (i.e the success and prediction rate curves) are produced only in the *geomode* because they require geographical data (shapefile) as additional input. A complete list of the output with a detailed description is provided in the supplementary material (LAND-SE_UserGuide.pdf).

3 LAND-SE applications

To show software functionalities and output types, LAND-SE was applied in a test area. Different configurations were selected to perform the following analysis:

- Polygon-based landslide susceptibility zonation;
- Pixel-based landslide susceptibility zonation;
- Landslide susceptibility scenarios zonation.

The applications use different mapping units and distinct schema to select the training and validation dataset. One analysis is focused to illustrate the use of LAND-SE to evaluate the impact of different scenarios of land use on LS. LAND-SE results can be considered relevant information in environmental planning and management.

3.1 Description of the example area and available data

A small area was selected to show applications and output of LAND-SE. The area is located in the eastern portion of the Briga catchment (Figure 2), in the Messina province (Sicily, South Italy). It has elevation values ranging from the sea level to about 500 m and terrain gradient in the range of 0° - 81° . Landslides, including shallow soil slides and debris flows, deep-seated rotational and translational slides, and complex and compound failures (Varnes, 1984), are abundant, and caused primarily by rainfall (Ardizzone et al., 2012; Reichenbach et al., 2014; 2015). On 1 October 2009, the Briga catchment and the surrounding areas were hit by an intense storm (Maugeri and Motta, 2011) that triggered more than 1000 shallow landslides, mainly shallow soil slides and debris flows (Varnes, 1984), caused 37 fatalities, numerous injured people and severe damages in the affected villages and along the transportation network.

After the event, a detailed landslide inventory map at 1:10,000 scale was prepared for the entire Briga catchment (Ardizzone et al., 2012). The inventory was obtained through a combination of field surveys carried out in the period from October to November 2009, and visual interpretation of pre-event and post-event stereoscopic and pseudo-stereoscopic aerial



210 photographs. The inventory map shows the distribution and types of landslides triggered by the
211 1 October 2009 rainfall event (Figure 2), and the distribution and types of pre-existing
212 landslides. In addition, two maps reporting the land use in different periods were prepared
213 exploiting available aerial photographs and Very High Resolution (VHR) satellite imagery
214 (Reichenbach et al., 2014; 2015). The first map was derived from the analysis of the same black
215 and white aerial photograph used to map pre-event landslides. The second map was obtained
216 from the analysis of two QuickBird satellite images taken the first on 2 September 2006 and
217 the second on 8 October 2009 (Mondini et al., 2011).

218 In the area, landslide susceptibility zonation were prepared using two mapping units: pixels and
219 slope-units. The slope-units (SU) are terrain subdivisions bounded by drainage and divide lines
220 (Carrara et al., 1991). SU were outlined using a 5-meter resolution DEM obtained resampling
221 the VH resolution DEM provided by the Italian national Department for Civil Protection and
222 using a recently developed *r.slopeunits* module (Marchesini et al., 2012; Alvioli et al., 2016).
223 The size and the geometrical characteristics of the SU are controlled by modeling parameters
224 defined by the user including the minimum half-basin area (Metz et al., 2011) and the slope
225 aspect variability. In the study area, the procedure identified 238 SU which represent the
226 polygon-based mapping units for the determination of LS. To explain the spatial distribution of
227 landslides (Carrara et al., 1991; 1995), for each slope-unit, we calculated the percentage of the
228 event landslides as dependent (grouping) variable and the following explanatory variables: i)
229 descriptive statistics (range, mean, standard deviation) of elevation and slope; ii) the percentage
230 covered by each land use class; and iii) the percentage covered by old landslides.

231 For the pixel-based analysis, we used the VH resolution DEM (1m x 1m) that accounts for
232 about 5 million cells. Maps of the elevation, slope, land use and of the presence/absence of old
233 landslides, were used as explanatory variables in the analysis. The presence/absence of event
234 landslides was used as dependent variable (Carrara et al., 1991, 1995; Guzzetti et al., 2006).
235 The data originally in polygon format were first converted in raster and all the data were
236 converted to the tabular format to be suited for LAND-SE (see LAND-SE_UserGuide.pdf for
237 details).

238



239 **3.2 Polygon-based landslide susceptibility zonation**

240 This example is focused to illustrate landslide susceptibility zonation prepared using the slope-
241 unit as mapping unit. Two spatial criteria were used to define the training and validation dataset,
242 the first based on a random selection and the second on the subdivision of the entire catchment
243 in two contiguous areas (Nord and South).

244 In the first case, the training set contained 70% of the total slope-units and the validation
245 corresponded to the entire basin. Landslide susceptibility models were trained using a subset of
246 available data and results were applied in validation to the entire study area. Figure 3 shows the
247 main graphical and geographical outputs obtained during the training and the validation phases,
248 including susceptibility, error and uncertainty maps, fourfold (contingency) plot, success and
249 prediction rate curves, ROC plot, evaluation and uncertainty plots. For simplicity, the figure
250 shows only results of the combined model, but outputs for each single model are available and
251 can be exploited for further analysis. In the example, the random selection criteria resulted in
252 similar training and validation performances (Figure 3). This application simulates LS zonation
253 for large territory, where landslides information is spotted and do not cover the entire study
254 area. In such conditions, training cannot be performed on the entire area and a random selection
255 of the training dataset, within the surveyed area, is a reasonable solution.

256 In the second case, the SU located in the Northern part of the Briga catchment with respect to
257 the main river, were used as training set and the SU located in the Southern portion as validation
258 set. Figure 4 shows outputs, including susceptibility maps for the combined model, success and
259 prediction rate curves, and ROC plots. As shown in Figure 4, the spatial subdivision resulted in
260 good model skill analysis, but reduced validation performances, underlying a poor spatial
261 exportability of the model (i.e. poor applicability of the resulting model coefficients to different
262 study areas). This type of application simulates LS zonation for areas where landslides
263 information required to train the model, is available only for a portion of the area. Results
264 obtained in the training phase are then applied to estimate susceptibility to the portion of the
265 territory where landslide data are not available. This application can be useful to evaluate the
266 possibility to use the same model output in different portion of territory or in different areas.

267 **3.3 Pixel-based landslide susceptibility zonation**

268 This example shows a landslide susceptibility zonation prepared using the pixel as mapping
269 unit. A random selection was chosen to prepare the training set and the validation was



performed applying results on the entire study area. For the purpose, in the training set all the pixels corresponding to landslides and an equal number of pixels in stable areas were selected. Figure 5 shows the main outputs of the combined model prepared for the entire area during the validation phase, including susceptibility, error and uncertainty maps, fourfold (contingency) plot, prediction rate curve, ROC plot, evaluation and uncertainty plots. This example simulates a common and widespread susceptibility zonation approach that exploits pixel-based analysis at basin and regional scale. In such conditions, reasonable calculation times with a limited loss of performances can be reached to training the model with a random selected subset and applying results to the entire study area. As shown in Figure 5, although the training was performed with a subset of the data, the model performance for the entire study area is adequate and acceptable.

3.4 Landslide susceptibility scenarios zonation

This example illustrates how LAND-SE can be utilized to evaluate the impact of different land-use scenarios on landslide susceptibility zonation (Reichenbach et al. 2014, 2015). The current, the past and possible future land-use distributions were evaluated on landslide susceptibility classes. Single models (linear discriminant analysis, quadratic discriminant analysis and logistic regression) and a combined model were prepared, exploiting the 2009 event landslides as grouping variable and morphological and land-use classes as explanatory variables.

To evaluate the influence of land use change on landslide susceptibility zonation, results obtained with the 2009 land use map were applied using the 1945 land use distribution. Figure 6 portrays on the left, the combined model prepared using the 2009 land use map, and on the right the zonation obtained applying the results to the 1954 land use cover. Moreover, to estimate the effect of land use distribution, we have designed different scenarios obtained changing the 2009 land use cover. Assuming an increase in the forested areas, we have considered three types of changes computed at the slope unit scale resulting in the following scenarios: i) 75% decrease in the pasture extent (Scenario 1); ii) 75% reduction of both pasture and cultivated areas (Scenario 2); and iii) 75% decrease in bare soil where the slope-unit mean angle was greater than 15° together with 75% decrease in pasture areas (Scenario 3). A fourth scenario was prepared assuming the effect of a forest fire in the south-west part of the area, where we simulated a reduction of the forested cover and an increase in bare soil (Scenario 4).



300 For each scenario, figure 7 shows the CM zonation and the success rate curve measuring the
301 fitting performance of each model.

302 Analyses of the scenarios confirm how land use changes significantly affect the spatial
303 distribution of unstable/stable slopes. This information can be used to evaluate the
304 consequences of land use change on vulnerability and risk. Moreover, the proposed approach
305 can be helpful to analyse the potential effects of land use planning and management on slope
306 instability.

307

308 **4 Final remarks**

309 A recent review analysis on landslide statistical models revealed a large variety of statistical
310 types, but a significant scarcity of a complete and comprehensive evaluation of the models
311 performance and prediction skills (Malamud et al. 2014). Moreover assessment of the input
312 data quality (Ardizzone et al. 2002), discussion on the scale applicability and the quantification
313 of errors and uncertainty associate to the models are limited. In the recent years there has been
314 an increase number of commercial and open source packages for statistical analysis that
315 integrate geographical data and/or Open Source GIS, but software dedicated to landslide
316 susceptibility zonation using statistical models is not available.

317 LAND-SE is an open source SW that performs LS modelling, zonation, results evaluation and
318 associated uncertainty estimation using graphs, map and statistical metrics filling the lacks of
319 the large variety of statistical methods already available. We think further improvements may
320 include additional models (i.e. forest tree analysis), tools for the input data preparation, tools
321 for the visualization of results available now only in textual format (i.e. test of the collinearity
322 evaluation, number of significant variables). Moreover, the software can be applied and
323 customized to different applications, providing the users with the possibility to implement and
324 improve the code with additional models, evaluations tools or output types. LAND-SE can also
325 be used to prepare models to predict particular types of slope movements (e.g. debris flow
326 source areas, Carrara et al., 2008) or can be customized to evaluate the probability of spatial
327 occurrence of completely diversified natural phenomena.

328

329 **Acknowledgements**



330 The implementation and improvement of LAND-SE with respect to the version published by
331 Rossi et al. (2010), was supported by the FP7 LAMPRE Project (Landslide Modelling and
332 Tools for vulnerability assessment preparedness and recovery management, EC contract n.
333 31238).

334

335 **Code availability and licence**

336 The LAND-SE code is provided as supplementary materials together with:

- 337 1. the software user guide (LAND-SE_UserGuide_v1_03mar2016.docx);
- 338 2. datasets containing the software script (LAND-SE_v30_20160118.R), the configuration
339 files (LAND-SE_configuration_spatial_data.txt, LAND-SE_configuration.txt) and input
340 files (training.txt, training.shp, validation.txt, validation.shp) relative to three examples
341 applications: (i) polygon-based landslide susceptibility zonation with a random selection
342 of the training dataset and a validation on a larger area; (ii) polygon-based landslide
343 susceptibility zonation with training and validation performed in two different contiguous
344 areas; (iii) pixel-based landslide susceptibility zonation with a random selection of the
345 training dataset and a validation on a larger area.

346 LAND-SE Copyright (C) Mauro Rossi. LAND-SE is free software; it can be redistributed or
347 modified under the terms of the GNU General Public (either version 2 of the License, or any
348 later version) as published by the Free Software Foundation. The program is distributed in the
349 hope that it will be useful, but WITHOUT ANY WARRANTY; without even the implied
350 warranty of MERCHANTABILITY or FITNESS FOR A PARTICULAR PURPOSE. See the
351 GNU General Public License for more details.

352

353

354 **References**

355 Alvioli, M., Marchesini, I., Reichenbach, P., Rossi, M., Fiorucci, F., Ardizzone, F., and
356 Guzzetti, F.: Automatic delineation of geomorphological slope-units and their optimization for
357 a selected landslide susceptibility model, Environmental Modelling & Software (under
358 revision), 2016.

359 Ardizzone, F., Basile, G., Cardinali, M., Casagli, N., Del Conte, S., Del Ventisette, C., Fiorucci,
360 F., Garfagnoli, F., Gigli, G., Guzzetti, F., Iovine, G., Mondini, A. C., Moretti, S., Panbianco,
361 M., Raspini, F., Reichenbach, P., Rossi, M., Tanteri, L., and Terranova, O.: Landslide inventory
362 map for the Briga and the Giampileri catchments, NE Sicily, Italy, Journal of Maps, 8:2, 176-
363 180, 2012.



- 364 Ardizzone, F., Cardinali, M., Carrara, A., Guzzetti, F., and Reichenbach P.: Impact of mapping
365 errors on the reliability of landslide hazard maps, *Natural Hazards and Earth System Sciences*,
366 2:1-2, 3-14, 2002.
- 367 Belsley, D.A.: *Conditioning diagnostics, collinearity and weak data in regression*, John Wiley
368 & Sons, New York, 1991.
- 369 Brabb, E. E.: *Innovative approaches to landslide hazard mapping*, *Proceedings 4th International*
370 *Symposium on Landslides*, Toronto, 1, 307-324, 1984.
- 371 Brown, C.E.: *Applied Multivariate Statistics in Geohydrology and Related Sciences*, Springer-
372 *Verlag*, Berlin, 248 pp., 1998
- 373 Carrara, A., Cardinali, M., Detti, R., Guzzetti, F., Pasqui, V., and Reichenbach, P.: GIS
374 techniques and statistical models in evaluating landslide hazard, *Earth Surface Processes*
375 *Landform*, 16:5, 427-445, 1991.
- 376 Carrara, A., Crosta, G., and Frattini, P.: Comparing models of debris-flow susceptibility in the
377 alpine environment, *Geomorphology*, 94:3, 353-378, 2008.
- 378 Carrara, A., Cardinali, M., Guzzetti, F., and Reichenbach, P.: GIS technology in mapping
379 landslide hazard, Carrara, A., Guzzetti, F. (eds.), *Geographical Information Systems in*
380 *Assessing Natural Hazards*. Kluwer Academic Publisher, Dordrecht, The Netherlands, 135-
381 175, 1995.
- 382 Chung, C.-J.F., and Fabbri, A.G.: Validation of spatial prediction models for landslide hazard
383 mapping, *Natural Hazards*, 30:3, 451-472, 2003.
- 384 Chung, C.-J.F., and Fabbri, A. G.: Probabilistic prediction models for landslide hazard
385 mapping, *Photogrammetric Engineering and Remote Sensing*, 65-12, 1389-1399, 1999.
- 386 Cohen, J.: A coefficient of agreement for nominal scales, *Educational and Psychological*
387 *Measurement*, 20, 37-46, 1960.
- 388 Cox, D.R.: The regression analysis of binary sequences. *Journal of the Royal Statistical Society*,
389 *Series B, Methodological* 20, 215–242, 1958.
- 390 Davison, A. C., and Hinkley, D.: *Bootstrap methods and their applications*, 8th ed., Cambridge
391 *Series in Statistical and Probabilistic Mathematics*, Cambridge University Press, ISBN-13:
392 9780521574716, 2006.
- 393 Efron, B.: Bootstrap methods: another look at the jack knife, *Annals Statistics* 7:1, 1-26, 1979.
- 394 Fawcett T.: An introduction to ROC analysis, *Pattern Recognition Letters*, 27:8, 861-874, 2006.
- 395 Felicísimo, Á., Cuartero, A., Remondo, J., and Quirós, E.: Mapping landslide susceptibility
396 with logistic regression, multiple adaptive regression splines, classification and regression trees,
397 and maximum entropy methods: a comparative study, *Landslides*, 10:2, 175-189, 2013
- 398 Fisher, R.A.: The use of multiple measurements in taxonomic problems, *Annales Eugenics* 7,
399 179–188, 1936.
- 400 Green, D. M., and Swets, J. M.: *Signal detection theory and psychophysics*, John Wiley and
401 *Sons*, New York. ISBN: 0-471-32420-5, 1966.
- 402 Guzzetti, F., Carrara, A., Cardinali, M., and Reichenbach, P.: Landslide hazard evaluation: a
403 review of current techniques and their application in a multi-scale study, Central Italy,
404 *Geomorphology*, 31: 181-216, 1999.



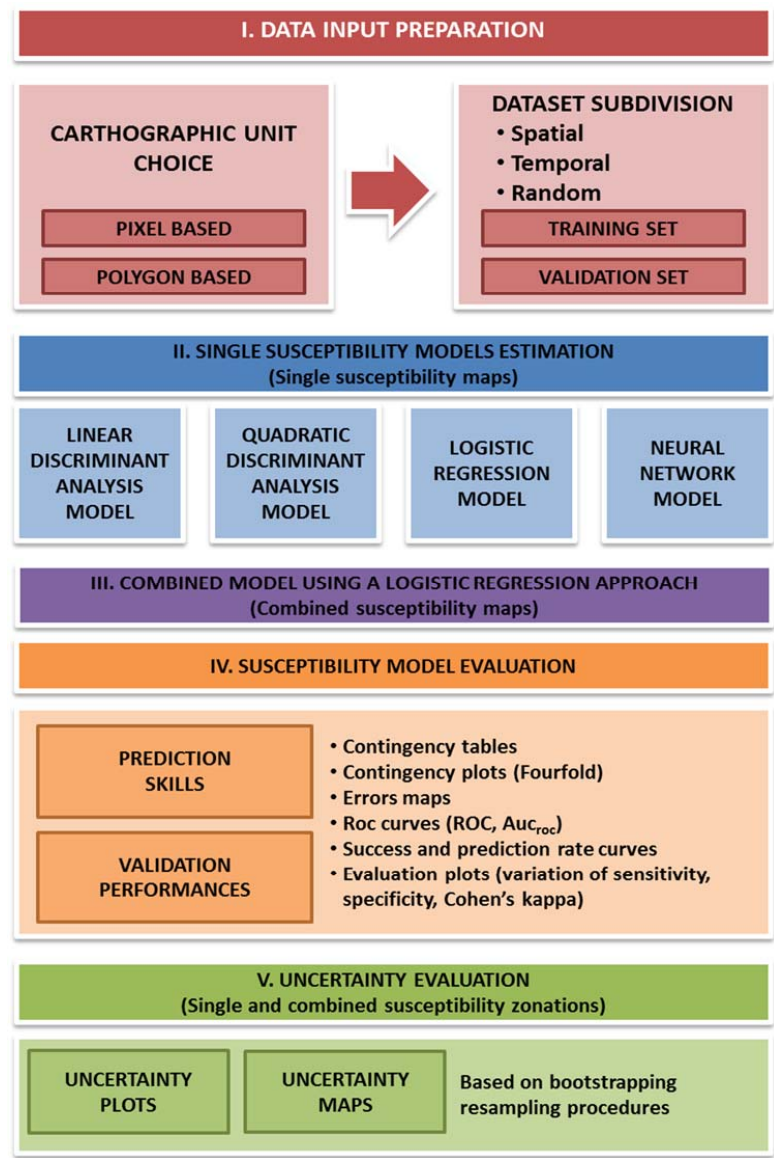
- 405 Guzzetti, F., Reichenbach, P., Ardizzone, F., Cardinali, M., and Galli, M.: Estimating the
406 quality of landslide susceptibility models, *Geomorphology*, 81:1-2, 166-184, 2006.
- 407 Jolliffe, I. T., and Stephenson, D. B.: *Forecast verification, A Practitioner's Guide in*
408 *Atmospheric Science*. John Wiley, Chichester, 240 pp, 2003.
- 409 Hendrickx, J.: *perturb: Tools for evaluating collinearity*. R package version 2.05.
410 <http://CRAN.R-project.org/package=perturb>, 2012.
- 411 Malamud, B., Mihir, M., Reichenbach, P., and Rossi, M.: D6.3-Report on standards for
412 landslide susceptibility modelling and terrain zonations, LAMPRE FP7 Project deliverables,
413 <http://www.lampre-project.eu>, 2014.
- 414 Marchesini, I., Alvioli, M., Rossi, M., Santangelo, M., Cardinali, M., Reichenbach, P.,
415 Ardizzone, F., Fiorucci, F., Balducci, V., Mondini, A.C., and Guzzetti, F.: WPS tools to support
416 geological and geomorphological mapping, OGRS 2012, Open Source Geospatial Research &
417 Education Symposium, October 24-26 2012, Yverdon-les-Bains, Switzerland,
418 <http://ogrs2012.org/index.php/ogrs2012/ogrs2012/paper/view/34>, 2012.
- 419 Mason, S. J., and Graham, N. E.: Areas beneath the relative operating characteristics (ROC)
420 and relative operating levels (ROL) curves: statistical significance and interpretation, *Quarterly*
421 *Journal of the Royal Meteorological Society*, 128, 2145-2166, 2002.
- 422 Maugeri, M., and Motta, E.: Effects of heavy rainfalls on slope behavior: the October 1, 2009
423 disaster of Messina (Italy), Iai, S. (ed.) *Geotechnics and Earthquake Geotechnics Towards*
424 *Global Sustainability*, Geotechnical, Geological and Earthquake Engineering 15, Springer
425 Science + Business Media, 2011.
- 426 Metz, M., Mitsova, H., and Harmon, R.: Efficient extraction of drainage networks from
427 massive, radar-based elevation models with least cost path search, *Hydrology Earth System*
428 *Science*, 15, 667-678, 2011.
- 429 Mondini, A. C., Guzzetti, F., Reichenbach, P., Rossi, M., Cardinali, M., and Ardizzone, F.:
430 Semi-automatic recognition and mapping of rainfall induced shallow landslides using optical
431 satellite images, *Remote Sensing of Environment*, 115:7, 1743-1757, 2011.
- 432 Owen, M., Imai, K., King, G., and Lau, O.: *Zelig everyone's statistical software*, R package
433 version 4.2-1, <http://CRAN.R-project.org/package=Zelig>, 2013.
- 434 Petschko, H., Brenning, A., Bell, R., Goetz, J., and Glade, T.: Assessing the quality of landslide
435 susceptibility maps – case study Lower Austria, *Natural Hazards Earth System Science*, 14:1,
436 95-118, 2014.
- 437 R Core Team: *R: A language and environment for statistical computing*, R Foundation for
438 Statistical Computing, Vienna, Austria, <https://www.R-project.org/>, 2015.
- 439 Reichenbach, P., Busca, C., Mondini, A. C., and Rossi, M.: Land use change scenarios and
440 landslide susceptibility zonation: the Briga catchment test area (Messina, Italy), *Engineering*
441 *Geology for Society and Territory*, 1, 557-561, Springer International Publishing, 2015.
- 442 Reichenbach, P., Busca, C., Mondini, A. C., and Rossi, M.: The influence of land use change
443 on landslide susceptibility zonation: the Briga catchment test site (Messina, Italy),
444 *Environmental Management*, 54:1372-1384, 2014.
- 445 Ripley, B.D.: *Pattern Recognition and Neural Networks*. InCambridge University Press, ISBN:
446 0-521-46086 7, pp. 416, 1996.



- 447 Rossi M., Guzzetti F., Reichenbach P., Mondini A. C., and Peruccacci S.: Optimal landslide
448 susceptibility zonation based on multiple forecasts, *Geomorphology*, 114:3, 129-142, 2010.
- 449 Van Den Eeckhaut, M., Marre, A., and Poesen, J.: Comparison of two landslide susceptibility
450 assessments in the Champagne–Ardenne region (France), *Geomorphology*, 115:1–2, 141-155,
451 2010
- 452 Varnes D. J.: IAEG Commission on Landslides: Landslide hazard zonation: a review of
453 principles and practice, 1984.
- 454 Venables, W.N., Ripley, B.D.: *Modern Applied Statistics with S*, Fourth edition, Springer,
455 Berlin, ISBN: 0-387-95457-0, pp. 495, 2002.
- 456



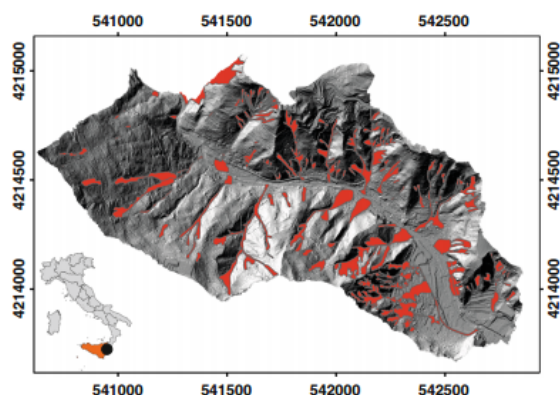
457 **Figures**



458

459

460 Figure 1. Logical schema of the LAND-SE software for landslide susceptibility modelling and
461 zonation.
462



463

464

465 Figure 2. Shaded relief of the study area located in the Briga catchment, along the Ionian coast
466 of Sicily (Italy). Red polygons show landslides triggered by the October 1, 2009 rainfall event.

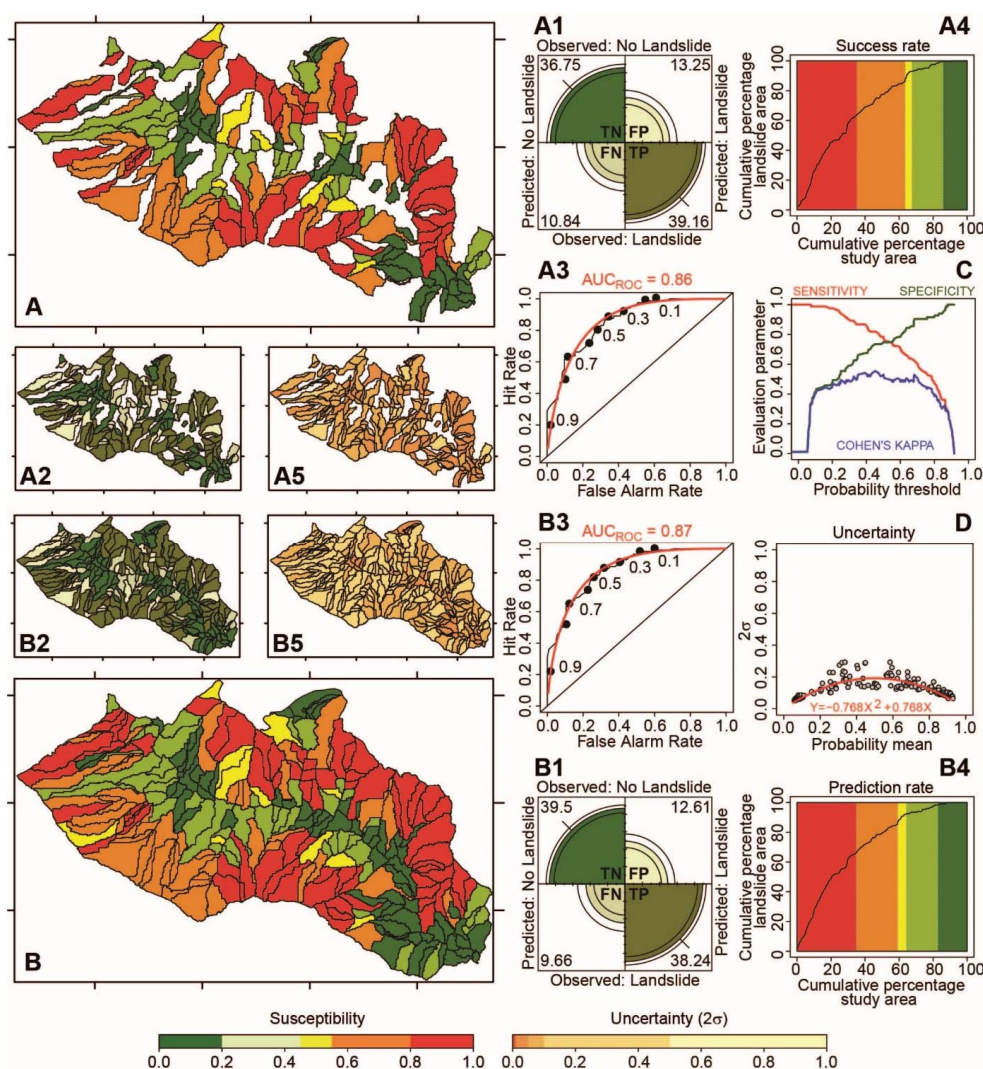


Figure 3. Landslide susceptibility maps (CM) for the training dataset (A) and the validation dataset (B) classified in five unequally spaced classes (see legend). (A1, B1) fourfold plots summarizing the number of true positives (TP), true negatives (TN), false positives (FP), and false negatives (FN); (A2, B2) maps of the distribution of the four categories of slope units reported in the fourfold plots; (A3, B3) ROC plots; (A4, B4) success and prediction rate curves; (C) variation in the model sensitivity, specificity, and Cohen's kappa index; (D) plot showing measures of the model error (2σ) vs. the mean probability (μ), for each slope unit, (black circle); (A5, B5) maps of the geographical distribution of the model error.

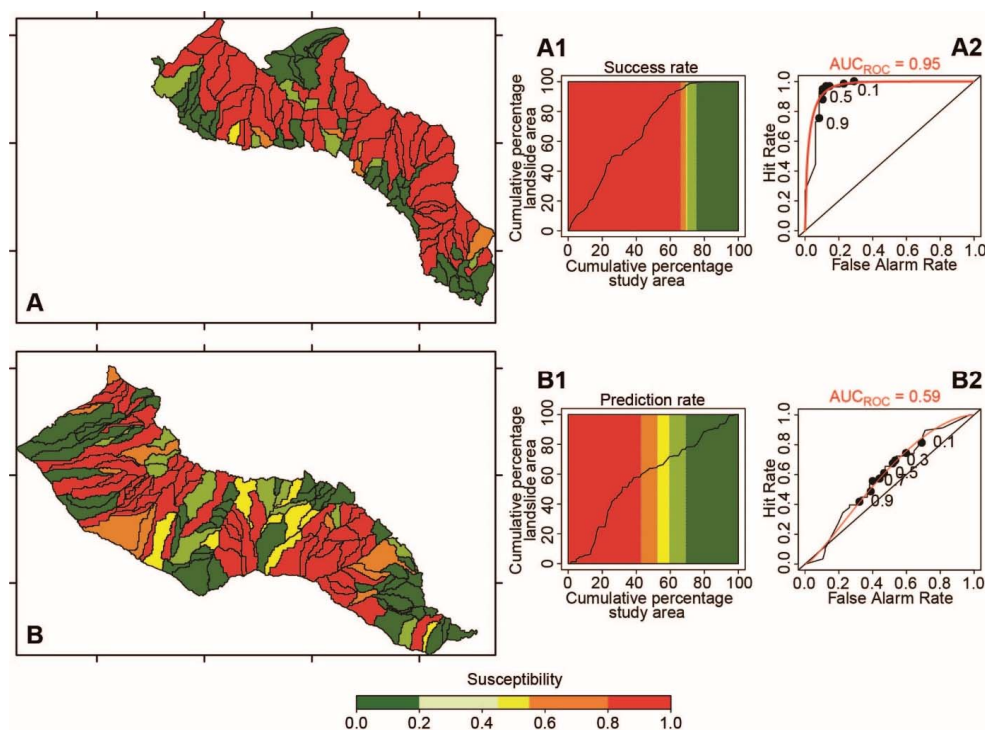


Figure 4. Landslide susceptibility maps (CM) for the training dataset (A: Northern part) and the validation dataset (B: Southern part) of the test area, classified in five unequally spaced classes (see legend). (A1, B1) success and prediction rate curves; (A2, B2) ROC plots.

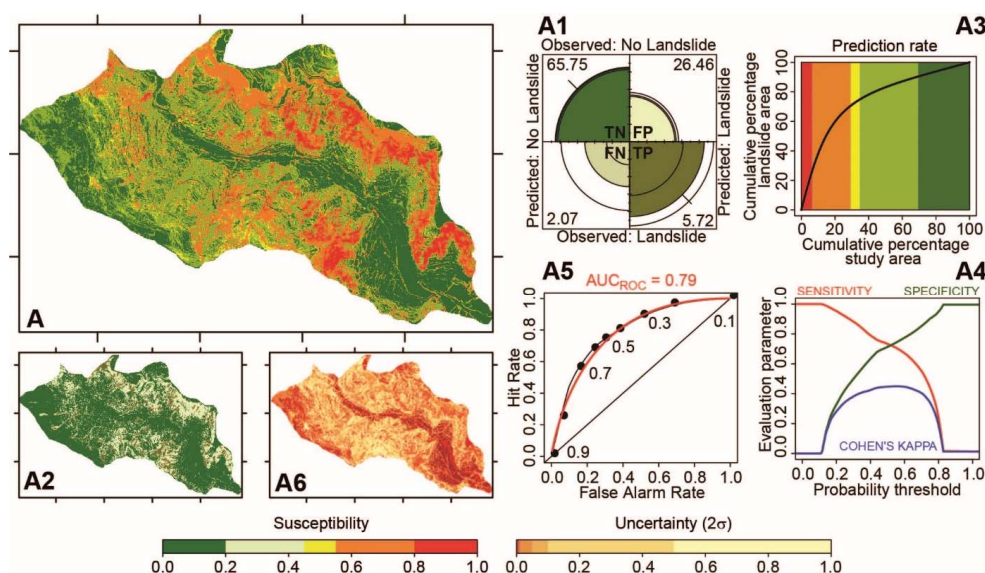


Figure 5. Pixel-based landslide susceptibility map (CM) of the test area (A) classified in five unequally spaced classes (see legend). (A1) fourfold plot summarizing the number of true positives (TP), true negatives (TN), false positives (FP), and false negatives (FN); (A2) map of the distribution of the four categories reported in the fourfold plot; (A3) prediction rate curve; (A4) variation in the model sensitivity, specificity, and Cohen's kappa index; (A5) ROC plot; (A6) map of the geographical distribution of the model error.

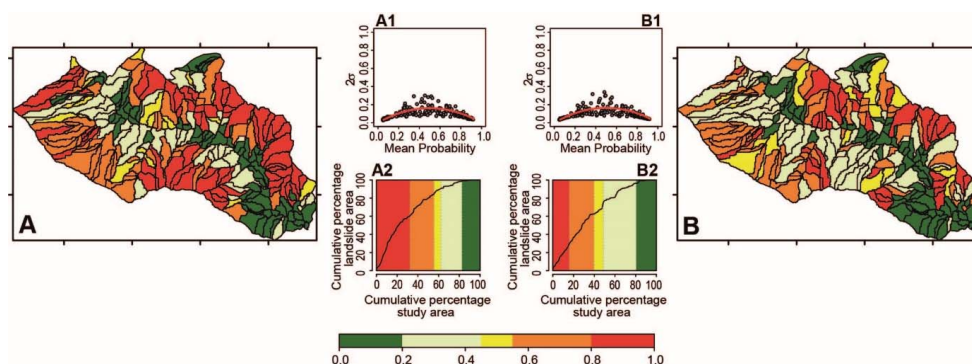
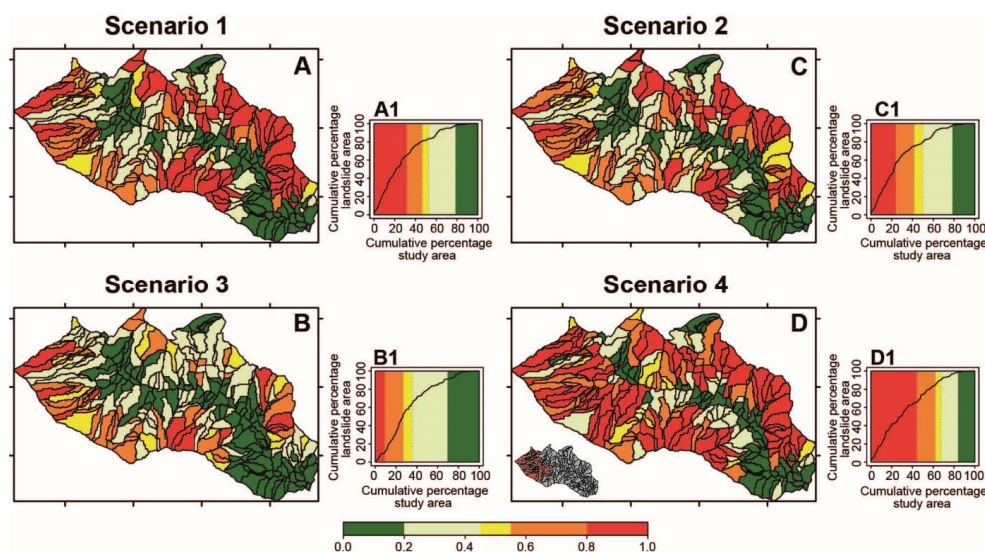


Figure 6. (A) Landslide susceptibility map (CM) prepared using the 2009 land use and (B) using the 1954 land use cover. LS maps are classified in five unequally spaced classes (see legend); (A1, B1) plot showing the model uncertainty estimated in each slope unit; (A2, B2) success rate curves.

494



495

496

497 Figure 7. (A, B, C, D) Landslide susceptibility maps (CM) classified in five unequally spaced
 498 classes prepared using different land use scenario; (A1, B1, C1, D1) success rate curves.